Proceedings of HT2005
2005 ASME Summer Heat Transfer Conference
July 17-22, 2005, San Francisco, California, USA

HT2005-72584

The effect of roughness on the impact dynamics and heat transfer of cryogen droplets impinging onto indented skin phantoms

Jie Liu,
Department of Mechanical Engineering
University of California, Riverside

Walfre Franco,
Department of Mechanical Engineering
University of California, Riverside

Guillermo Aguilar
Department of Mechanical Engineering
University of California, Riverside

Keywords: Cryogen droplet, skin phantom, heat transfer

ABSTRACT

Laser dermatological surgery (LDS) is the preferred therapeutic modality for various dermatoses, including port wine stain (PWS) birthmarks. LDS is commonly used in conjunction with cryogen spray cooling, which is an auxiliary procedure that pre-cools the superficial skin layer (epidermis) prior to laser irradiation to avoid non-specific and excessive epidermal heating. Clinical observations show that skin indents markedly during spray deposition due to the large momentum of cryogen droplets. Furthermore, the human skin surface is far from smooth. Therefore, with the objective to provide some insight into the interaction between cryogen sprays and the rough and deformable human skin surface, the impingement dynamics and heat transfer induced by single cryogen droplets falling on rough and indented skin phantoms are present in this paper. Epoxy skin phantoms with a constant semispherical indentation of depth and radius of 2.44 mm and 6.34 mm, respectively, were used to simulate indented skin. Each phantom had a different surface roughnesses varying from 0.5 μm to 50 μm. The experiments were carried out within a pressurized chamber to control or eliminate droplet evaporation. A high-speed camera and the temperature sensors placed on the upper surface of the skin phantoms were synchronized to record the impact dynamics and temperature changes as cryogen droplets fell on them. The results show that the surface roughness affects the impact dynamics and heat transfer during single droplet impingement. As the surface roughness (*Ra*) increasing, the heat flux decrease.

NOMENCLATURE

A_s	maximum covered area of spread [mm^2]
A_r	covered area after retreat [mm^2]
C_d	drag coefficient
d_o	outer diameter of nozzle [mm]
D	diameter of droplet [mm]
d	depth of indentation [mm]
g	gravity [ms^2]
r	radius of indentation [mm]
Ra	Surface roughness [μm]
Re	Reynolds number ($\rho VD/\eta$)
t	time [ms]
t_s	spread time [ms]
t_r	retreat time duration [ms]
T_{sat}	saturation temperature [^{o}C]
V	droplet velocity [m/s]
V_b	break up velocity of droplet [m/s]
We	Webber number ($D\rho V^2/\sigma$)
η	dynamic viscosity [N s/m^2]
σ	surface tension [N/m]

INTRODUCTION

Laser dermatological surgery is the treatment of choice for cosmetic (e.g., hair [1] and tattoo [2] removal) as well as for vascular lesions (e.g., hemangiomas [3] and port wine stain (PWS) birthmarks [4]). For many of these treatments, cryogen spray cooling (CSC) is an essential auxiliary method that protects the epidermis from excessive thermal damage during laser irradiation, while the intended

target, such as hypertrophic blood vessels located 100–500 μm below the skin surface [5,6] are thermally photocoagulated. The only cryogen used for this purpose, approved by the FDA [6] is Tetrafluoroethane-1,1,1,2 (R134a), with a boiling temperature of -26 ^{o}C at ambient pressure. Short cryogen spurts (20–100ms) [6] are released from a pressurized container through a spray valve/nozzle system. Well-atomized cryogen droplets with diameters ranging between 3–20 μm [7] and velocities 10–60 m/s [8] impinge onto human skin and extract heat as they spread and evaporate.

The efficiency of the heat extraction during spray deposition is largely dictated by the dynamics of droplet impingement [9]. Moreover, during CSC, the momentum of the spray droplets causes skin indentations al large as 2 mm in depth. In a previous study, we investigated the effect of skin indentation on the heat extraction during CSC [11] using indented and smooth skin phantoms. It was seen that the maximum heat flux could be diminished by as much as 30% on phantoms with indentations of $\approx$ 2 mm in depth. Evidently, human skin surface is not smooth and its roughness (typically between 50 to 150 μm depending on anatomical location, age, race, etc. [10]) is likely to influence the efficiency of the heat extraction. Therefore, to better understand how CSC efficiency may be optimized, we decided to investigate single cryogen droplet impingement dynamics and its relationship to the heat extraction using indented and rough human skin phantoms.

EXPERIMENTAL SET UP

High pressure chamber and nozzle

To simplify the analysis of data and to either eliminate or control the evaporation rate of cryogen droplets we carry out our experiments within a custom-made high pressure aluminum chamber, schematically represented in Fig. 1. Prior to the experiments, the chamber was pressurized to 6.21 bar (T_{sat}=27 ^{o}C), which is higher than the saturation pressure of cryogen (R-134a) at room temperature (5.71 bar). To reduce further the evaporation during droplet impingement at this pressure, ice bags were wrapped around the chamber, reducing the inside chamber temperature to 10 ^{o}C.

Two transparent windows made of polycarbonate positioned on the two lateral ends of the chamber were used for illumination and imaging. The impact surface was held by one 5 × 5 cm Teflon insulation chamber that had a 2.5 × 2.5 cm electronic heater mounted at the bottom. The temperature of the heater was controlled by one Omega CSC32 bench top controller (OMEGA Engineering Inc., Stanford, CT). Between the heater and the phantom, one aluminum disc with 3 cm in diameter and 6 mm in thickness was used to diffuse the heat evenly to the skin phantom. The whole arrangement was horizontally mounted at the bottom of chamber.

Falling droplets were formed at the tip of small nozzles, which were attached to a control valve connected to a small cryogen tank pressurized slightly above the chamber's pressure (6.42 bar). For these experiments, the droplet diameter (D) and impact velocity (V) were kept constant at 1.9 mm and 2.0 m/s, respectively. For proper comparison and analysis, it was necessary to maintain similarity between the small (3–20 μm) and fast (10–60 m/s) cryogen spray droplets and the larger but slower droplets we generate within the chamber. For that purpose, we verified that the two most relevant dimensionless numbers, namely, the Weber ($We=D\rho V^2/\sigma$, where D is the droplet diameter, ρ is the density, V is the impact velocity and σ is the surface tension) and Reynolds ($Re=\rho VD/\eta$, where η is droplet viscosity), were equivalent. For spray droplets, typical values of Re and We at the point of impact are within the range of 600–24000 and 150–8000, respectively [7].

Imaging system

A high speed camera (Photron Fastcam PCI 10K, Itronics, Westlake Village, CA) was used to acquire digital images of single droplet impingement on the skin phantoms. Image sequences were captured at a rate of 1000 frames per second and pixel resolution of 128 × 120. To directly observe the impact dynamics and its relationship to the heat transfer phenomena, the pictures and the temperature profiles were synchronized by a custom-made Labview (National Instruments, Austin, TX) program. Two Fiber-Lite illuminators (Edmund Industrial Optics, Barrington, NJ) were used as light sources, one in front and the other on the back of the chamber. To record droplet impingement dynamics, the camera was positioned at a 30^{o} angle with respect to the horizontal. Droplet velocity was obtained using Motion software (Itronics, Westlake Village, CA) by comparing the same droplet in series of consecutive frames.

The velocity at which falling droplets break into smaller ones due to drag forces is known as, breakup velocity, which may be expressed as $V_b = 8\sigma/C_d\rho_{air}D$, where C_d is the drag coefficient. It was found that the chosen impact velocity of 2.0 m/s was far below the V_b for both droplet sizes studied herein.

Impact surfaces and data acquisition system

Three epoxy skin phantoms with skin-like thermal properties and same indentation geometry (radius r = 6.34 mm and depth d = 2.44 mm) [11], but each with different surface roughness (Ra): 0.5, 20 and 50 μm, respectively, were used. The one with Ra = 50 μm is the closest to human skin surface roughness [10]. The thermal sensor was made of a round silver disc of 3 mm in diameter and, 0.1 mm thick, welded to a miniature K-type thermocouple (OMEGA Engineering Inc., Stanford, CT) with bead diameter of 0.5 mm. The silver discs were made such that they maintained the same surface roughness and curvature of the epoxy phantom surface. The thermocouple was connected to SCB-68 data acquisition system (National Instruments) to record the temperature change during the impact process. For these experiments, we preset the skin phantom at two different initial temperatures: 10 ^{o}C and 25 ^{o}C, respectively, for both of which no boiling occurs at the chamber preset pressure (6.21 bar and T_{sat} = 27 ^{o}C). The measured temperature of the droplets at the time of impact was always –10 ^{o}C, to ensure an initial temperature differential of at least 20 ^{o}C between the falling droplets and the phantom surface. The choice of skin phantom and environmental temperatures at 10 ^{o}C was made with the purpose of minimizing a temperature differential between the droplets and the local environment and, thus, pronounced in-flight evaporation rate. For droplets falling with initial temperature of 25 ^{o}C, which is close to the nucleation boiling temperature (27 ^{o}C) at the preset pressure (6.21 bar), we expected to observe a

somewhat larger influence of the environment on the droplet evaporation rate. The heat flux at the phantoms surface was calculated by an inverse heat conduct (IHC) algorithm [8], which uses the recorded surface temperature.

RESULTS AND ANALYSIS

Once the droplet impinges onto a hard flat surface, the droplet deforms and spreads along the impact surface due to the kinetic energy before impact. After spreading to the maximum covered area (A_s), the droplet retreats or shrinks due to surface tension [12]. A similar phenomenon is observed when a droplet impinges onto an indented surface. Figures 2–4 show sequences of droplet impingement onto the three indented surfaces, respectively. Notice that the surface with Ra = 0.5 μm (Figure 2) shows the strongest impact dynamics, with portions of the droplet splashing outside the indentation rim. Once the spherical droplet impinges on the bottom of the indented surface, the cryogen spreads along the indentation over a spread time (t_s) lasting 2–8 ms and reaches A_s at 8 ms after impact. After reaching A_s, the cryogen begins to shrink back to the bottom of the indentation or the origin of the impact due to the surface energy and gravity. The retreat duration time (t_r) is much longer than t_s, and it reaches minimum covered area (A_r) at 140 ms. In Figure 3, (Ra = 20 μm), the droplet shows similar impact dynamics and reaches A_s at t_s = 8 ms and t_r is 140 ms. We can see that A_s in this case is smaller than that of Ra = 0.5 μm. For Ra = 50 μm (Figure 4), t_s = 8 ms is similar to the previous two cases, but it has the smallest A_s. The behavior of the droplets after spreading to the A_s are much different for the three surfaces too. With the smoothest surface (Ra = 0.5 μm) almost all the droplet retreats to the bottom of the indentation with the smallest A_t. As the surface roughness increases to 20 μm, the cryogen droplet does not retreat completely to the bottom and A_r is larger than that of Ra = 0.5 μm. For R_a = 50 μm, only a small portion of the droplet retreats to the bottom and most of it sticks to the surface once it has spread to that location.

The temperature profiles demonstrate how these surface roughnesses affect the heat transfer. Figure 5 shows the surface temperatures measured during droplet impingement onto the three rough indented surfaces as the substrates initial temperature is set to 10 ^{o}C. This figure shows that the temperature for Ra = 0.5 μm drops lower than that that of the rougher surfaces. The lowest temperature reached is 2.5, 5 and 6^{o}C for Ra = 0.5, 20 and 50 μm, respectively. Since the skin phantom has the same initial temperature than the ambient temperature, it is assumed that the effect of droplet evaporation is negligible.

Figure 6 shows similar experiments where the surface initial temperature is increased to 25 ^{o}C. Again, for Ra = 0.5 μm, the temperature drops lower than for the Ra = 20 μm and Ra = 50 μm cases. The lowest temperatures reached are 13, 17 and 16.5 ^{o}C for Ra = 0.5, 20 and 50 μm, respectively.

Figure 7 shows the heat flux during the impingement for the three different surface roughnesses and the skin phantom initial temperature of 10 ^{o}C. The surface with Ra = 0.5 μm shows the maximum heat flux of all (500 W/m^2). The heat fluxes for Ra = 20 and 50 μm are close to each other, but only reach a maximum of 375 W/m^2.

Figure 8 shows the heat flux during the impingement for the three different surface roughnesses and the skin phantom temperature of 25 ^{o}C. Again, this figure shows the highest heat flux of all (700 W/m^2) for the surface with Ra = 0.5μm and the maximum heat fluxes for the surfaces with Ra = 20 and 50 μm are close to each other but only reach 550 W/m^2.

From the comparison of the pictures of droplet impingement dynamics, the temperature profiles and the heat flux computations, it appears that the surface roughness affects the impingement dynamics and consequently the heat transfer. For the surface with Ra = 0.5 μm, there is a more violent impact and the A_s is the largest, while A_r is the smallest after the droplet retreats. That means that it has the maximum spread velocity during t_s and that most of the droplet mass deposits at the bottom of the indentation after the cryogen retreats. We speculate that high cryogen spread velocities help to increase the heat transfer by convection during the impingement and spreading process. After the retreat, the cryogen droplet still has a sufficiently low temperature and covers fully the sensor area, which translates into an efficient heat transfer process without boiling. The extreme case occurs for Ra = 50 μm, which has the smallest A_s and largest A_r. That means that for the same t_s, the spread velocity for Ra = 50 μm is the lowest and the mass of cryogen that covers the thermal sensor after retreat is the smallest. Therefore, the heat extraction by convection during the impingement and spreading process is not as efficient as for Ra = 0.5 μm.

The heat flux profiles reflect the cooling efficiency of the impingement and spreading process. In this experiment, the size of the thermal sensor is small (3 mm in diameter) compared to the size of the skin phantom and A_s. Therefore the heat flux can be calculated by using the 1-D IHC algorithm based on the surface temperature variation. It is apparent that surface roughness affects the heat flux greatly which is enhanced 20 % and 30 % as for skin phantom initial temperatures of 10 ^{o}C and 25 ^{o}C, respectively, as Ra decreases from 50 μm to 0.5 μm.

CONCLUSIONS

For the same indented geometry, the heat transfer phenomena are affected by the impact dynamics. For droplets with the same diameter, velocity and environmental conditions, the surface roughness affects the heat transfer through changing the impact dynamics. The lesser the surface roughness (Ra) the stronger the impact dynamics and the higher the heat flux. A practical consequence of these results is that more efficient CSC could be achieved by reducing the skin surface roughness, which would ultimately lead to a better outcome in many dermatologic laser therapies.

REFERENCES

1. Altshuler GB, Zenzie HH, Erofeev AV, Smirnov MZ, Anderson RR and Dierickx C, 1999, “Contact cooling of the skin”, Phys Med Biol, Vol. 44(4), 1003-1023.

2. Fitzpatrick RE and Goldman MP, 1994, “Tattoo removal using the alexandrite laser”, Arch. Dermatol, Vol. 130, 1508-1514.

3. Chang CJ, Anvari B and Nelson JS, 1998, “Cryogen spray cooling for spatially selective photocoagulation of

hemangiomas: A new methodology with preliminary clinical reports", Plast Reconstr Surg, Vol. 102, 459-463.

4. Nelson JS, Milner IE, Anvari B, Tanenbaum BS, Kimel S, Svaasand LO, and Jacques,SL,1995, "Dynamic epidermal cooling during pulsed laser treatment of port wine stain. A new methodology with preliminary clinical evaluation", Arch. Dermatol, 133, 695-700.

5. Nelson JS, Milner IE, Anvari, B, Tanenbaum, BS, and et al, 1994, "Dynamic epidermal cooling in conjunction with laser-induced photothermaloysis of port wine stain blood vessels", Lasers Surg. Med., Vol.19, 224-229.

6. Aguilar G, Majaron B, Verkruysse W, Zhou Y, Nelson JS, Lavernia EJ, 2001, "Theoretical and experimental analysis of droplet diameter, temperature, and evaporation rate evolution in cryogenic sprays", Intl. J Heat and Mass Transfer, Vol. 44 (17), 3201-3211.

7. Aguilar G, Majaron B, Pope K, Svaasand LO, Lavernia EJ, Nelson JS**,** 2001**, "**Influence of nozzle-to-skin distance in cryogen spray cooling for dermatologic laser surgery", Lasers Surg. Med, Vol. 28 (2), 113-120.

8. Aguilar G, Majaron B, Karapetian E, Lavernia EJ, Nelson JS**,** 2003, "Experimental study of cryogen spray properties for application in dermatologic laser surgery", IEEE Trans. On Biomedical Engineering, 50 (7), 863-869.

9. Aguilar G, Wang GX, Nelson JS, 2003, "Dynamic behavior of cryogen spray cooling: Effects of spurt duration and spray distance", Lasers Surg. Med, Vol. 32 (2), 152-159.

10. Manuskiatti, W, Schwindt, DA. And Maibach, HI., 1998, " Influence of age, anatomic site and race on skin roughness and scaliness", Dermatology, 196,401-407

11. Basinger B, Aguilar G and Nelson JS, 2004, "Effect of skin indentation on heat transfer during cryogen spray cooling", Lasers Surg. Med. Vol. 34 (2), 155-163.

12. Mao T, Kuhn DCS, Tran H**,** 1997, "Spread and rebound of liquid droplets upon impact on flat surfaces", AICHE JOURNAL, 43 (9), 2169-2179.

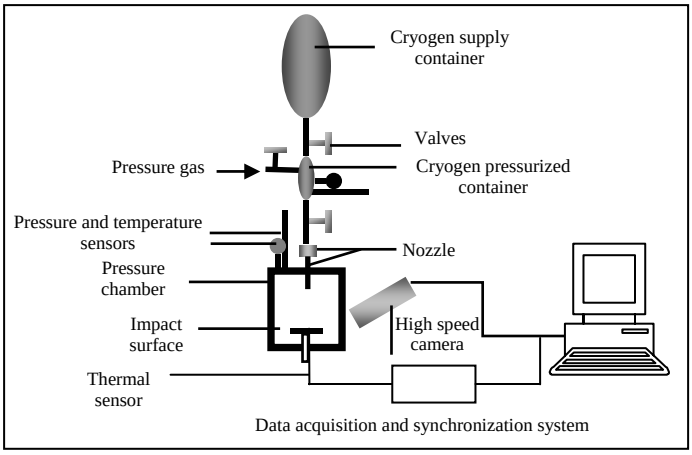

Figure 1. The experimental facilities

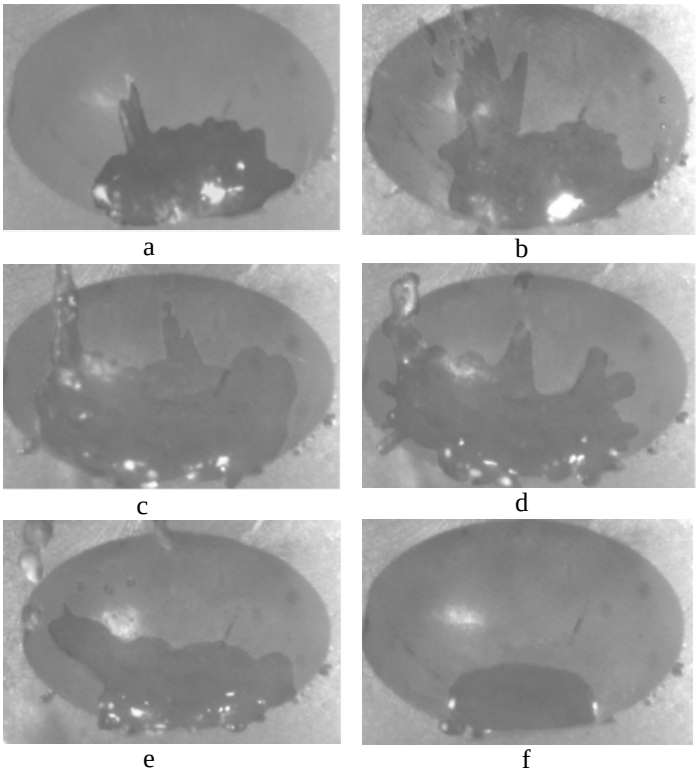

Figure 2. Droplet impingement onto to indentation with surface roughness Ra = 0.5 μm, with time sequence: a. t = 0.0, b. t = 2, c. t = 4, d. t = 8, e. t = 12 and f. t = 140 ms respectively

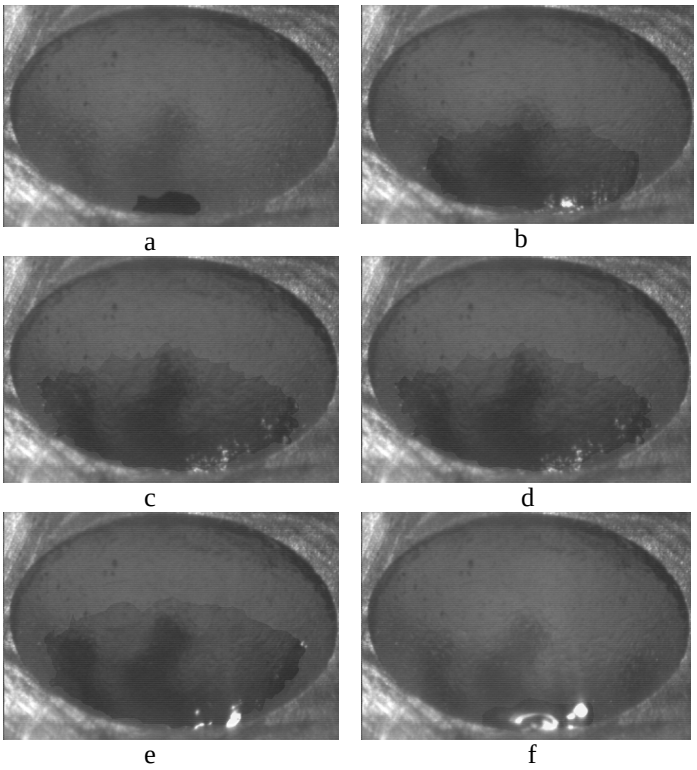

Figure 3. Droplet impingement onto to indentation with surface roughness 20 μm, with time sequence: a. t = 0, b. t = 2, c. t = 4, d. t = 8, e. t = 12 and f. t = 140 ms respectively.

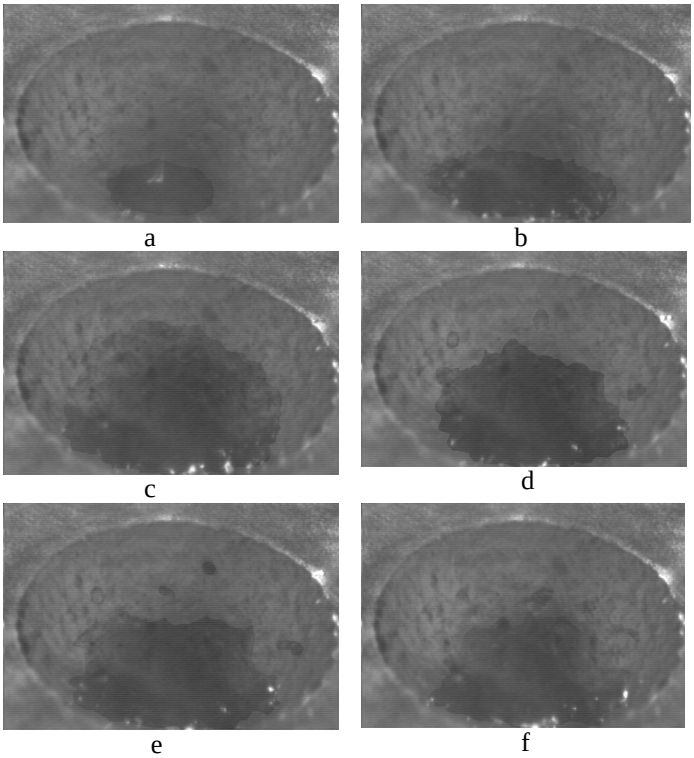

Figure 4. Droplet impingement onto to indentation with surface roughness 50 μm with time sequence: a. t = 0, b. t = 2, c. t = 4, d. t = 8, e. t = 12 and f. t = 140 ms respectively.

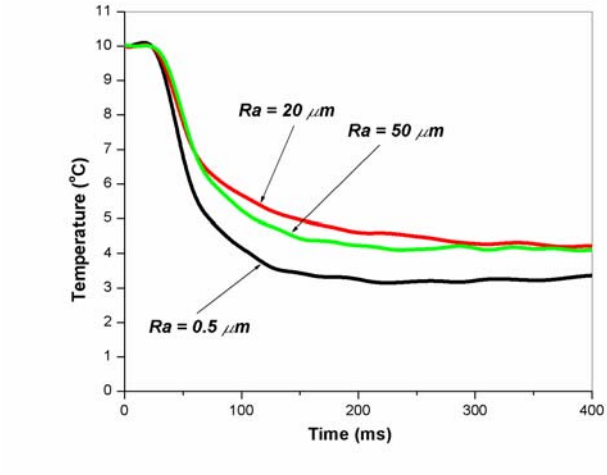

Figure 5. Temperature profile comparison between surface roughness *Ra* = 0.5 μm, *Ra* = 20 μm and *Ra* = 50 μm with environmental temperature is 10 ^{o}C and surface temperature 10 ^{o}C.

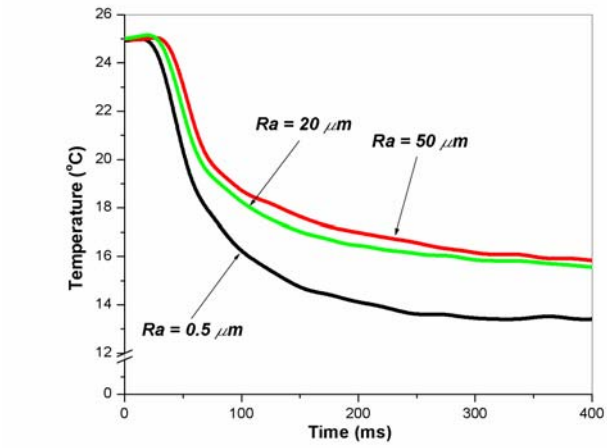

Figure 6. Temperature profile comparison between surface roughness *Ra* = 0.5 μm, *Ra* = 20 μm and *Ra* = 50 μm with environmental temperature is 10 ^{o}C and surface temperature 25 ^{o}C

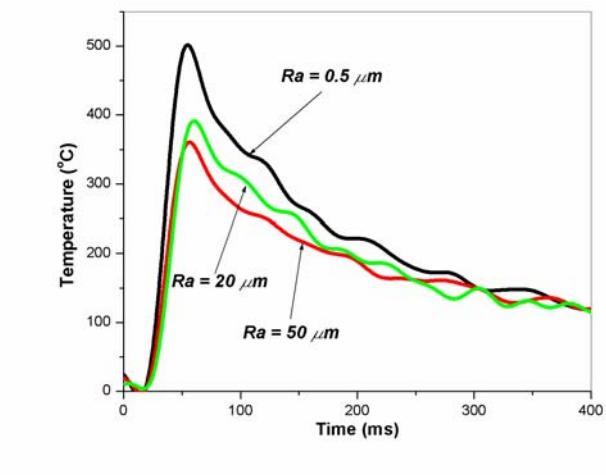

Figure 7. Heat flux profile comparison between surface roughness *Ra* = 0.5 μm, *Ra* = 20 μm and *Ra* = 50 μm with environmental temperature is 10 ^{o}C and surface temperature is 10 ^{o}C.

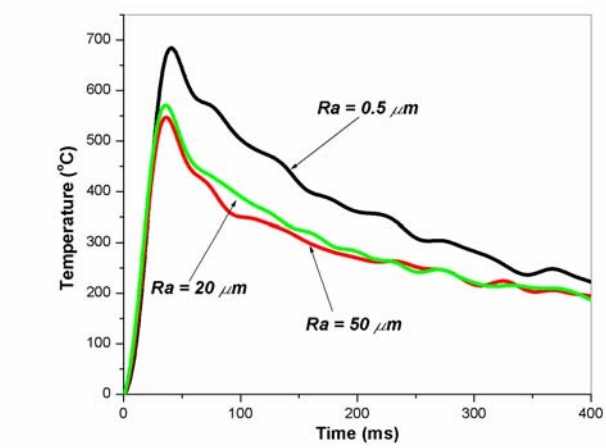

Figure 8. Heat flux profile comparison between surface roughness *Ra* = 0.5 μm, *Ra* = 20 μm and *Ra* = 50 μm with environmental temperature is 10 ^{o}C and surface temperature is 25 ^{o}C.